

Development of a parameterization for simulating the urban temperature hazard using satellite observations in climate model

Menglin Jin · J. Marshall Shepherd · Christa Peters-Lidard

Received: 20 September 2006 / Accepted: 13 February 2007
© Springer Science+Business Media B.V. 2007

Abstract Urban surface temperature is hazardously higher than surrounding regions (so-called urban heat island effect UHI). Accurately simulating urbanization-induced temperature hazard is critical for realistically representing urban regions in the land surface-atmosphere climate system. However, inclusion of urban landscapes in regional or global climate models has been overlooked due to the coarse spatial resolution of these models as well as the lack of observations for urban physical properties. Recently, National Aeronautics and Space Administration (NASA) Earth Observing System (EOS) Moderate Resolution Imaging Spectroradiometer (MODIS) observations illustrate important urban physical properties, including skin temperature, surface albedo, surface emissivity, and leaf area index. It is possible to identify the unique urban features globally and thus simulate global urban processes. An urban scheme is designed to represent the urban-modified physical parameters (albedo, emissivity, land cover, roughness length, thermal and hydraulic properties) and to include new, unique physical processes that exist in urban regions. The urban scheme is coupled with National Center for Atmospheric Research (NCAR) Community Land Model Version 2 (CLM2) and single column coupled NCAR Community Atmosphere Model CAM2/CLM2 to assess the mechanisms responsible for UHI. There are two-steps in our model development. First, satellite observations of albedo, emissivity, LAI, and *in situ* observed thermal properties are updated in CLM2 to represent

M. Jin (✉)
Department of Meteorology, University of Maryland,
College Park, NASA-GSFC Code 612.2,
Greenbelt, MD 20771, USA
e-mail: mjjin@atmos.umd.edu

J. M. Shepherd
Department of Geography, Atmospheric Sciences Program,
Physical Meteorologist/Climatologist, The University of Georgia,
Athens, MD, USA

C. Peters-Lidard
Hydrological Sciences Branch, Goddard Space Flight Center,
NASA, Greenbelt, MD, USA

the first-order urban effects. Second, new terms representing the urban anthropogenic heat flux, storage heat flux, and roughness length are calculated in the model. Model simulations suggest that human activity-induced surface temperature hazard results in overlying atmosphere instability and convective rainfall, which may enhance the possibility of urban flood hazard.

Keywords Urban system · Surface temperature hazard · Climate modeling

1 Introduction

The modern urbanization effect requests special attention since its rapid growth induces the changes in climate and weather conditions (Oke 1982; Karl et al. 1988; Hansen et al. 2001; Jin et al. 2005a, Jin and Dickinson 2000). Urban surface temperature is generally higher than that of the surrounding regions due to surface albedo decreases, surface vegetation reduction, and less soil moisture content over sealed concrete surfaces. By changing surface convection and local/regional atmospheric circulation, urban-related thermodynamic and dynamic forcing may be responsible, at least partly, for lightning hazards (Orville et al. 2001), flood hazards (Burian and Shepherd 2005; Burian et al. 2004; Bornstein and Lin 2000); pollution (Jauregui 1997; Rosenfeld 2000; Jin et al. 2005b) and thus affects human health (Kunkel et al. 1996). The United States Climate Change Science Program explicitly highlights the need for research on climatic effects of temperature on air quality, particularly in urban heat islands and other regional settings, and the potential health consequences (Shepherd 2005).

Global climate models (GCM), which include an atmospheric model coupled with land surface models, are useful tools to examine climate changes (IPCC 2001). The land surface model in a GCM simulates terrestrial water, energy and biogeochemical processes as well as the transfers of heat, mass and momentum between the land surface and the overlying atmosphere of the model. Unfortunately, simulating urban effects is one of the weakest aspects of current land surface models, because most were developed for coarse-resolution (e.g., about 100 km resolution) global models within which urban processes and impacts were once thought to be unimportant. Further, understanding of urban properties and physical processes is still incomplete (Jin and Shepherd 2005).

Our paper introduces an urban scheme to enhance currently existing land surface models for better simulating the urban temperature hazard and to examine its impact on energy and water balances. The strength of the scheme is its combining recently available Earth Observing System (EOS) satellite observations with existing land surface models to include urban landscape in the model (King et al. 2003). We hope to shed light on three key questions:

- (1) What are the physical mechanisms responsible for the urban temperature hazard (e.g. urban heat island effect)?
- (2) What is the relative importance of the mechanisms?
- (3) What are the impacts of the urban temperature hazard on the local water cycle?

Emphasizing the urban temperature hazard, we simulate land surface energy budgets and purposely ignore other processes including momentum changes over urban buildings. A detailed model for simulating urban momentum exchange is given by Otte et al. (2004). In

addition, we also neglect urban atmospheric aerosol and cloud anomalies, in particular, diurnal, weekly, seasonal variations and their impact on surface insolation and cloud formation processes (Jin et al. 2005b; Mölders and Olson 2004). This is justified partly because our model is a land surface scheme and modeling aerosol-cloud-land surface interaction is not our scope. Nevertheless, these factors do not affect the conclusions of this study.

The urban temperature hazard is determined by the land surface energy budget, which is the basis of all modern land surface models:

$$(1 - \alpha)S \downarrow + LW \downarrow - \varepsilon T_{\text{skin}}^4 - SH - LE - G = 0, \quad (1)$$

where SH is sensible heat flux, LE is latent heat flux, G is the ground heat flux. These three processes compete for surface net radiation, which is the downward minus upward shortwave and longwave radiation (the first 4 terms in Eq. (1)). In Eq. 1, is surface albedo, and S is downward solar radiation, therefore, $(1 - \alpha) S \downarrow$ is reflected solar radiation. $LW \downarrow$ is downward longwave radiation from the surface. Emissivity (ε) and surface skin temperature (T_{skin}) determine the upward longwave radiation, or surface emission, following the Stefan–Boltzmann Law. It is evident that urban modifications on α and ε play important roles in surface temperature changes since the net radiative energy are changed in land surface system (Jin et al. 2005a). In addition, the heights of buildings make the surface “roughness length” increase and thus SH and LE are affected by enhanced surface turbulence. Furthermore, urban paved roads and concrete surfaces are impervious and therefore paved surfaces lead to high Bowen ratios.

In addition to Eq. 1, which is valid for natural landscape, urban landscapes need two new terms in the surface energy budget: (1) anthropogenic heat flux attributed to fuel combustion, air conditioning, and other human activities (Grimmond and Oke 1999); and (2) storage heat flux due to heat emitted from vertical surfaces such as building walls (Oke 1982). Our scheme emphasis on including urban system in Eq (1) via modified physical parameters and new subroutine representing the new physical processes unique on urban system.

The following section introduces the data and model that we will use in this work. Section 3 discusses how the urban scheme we developed. Section 4 gives model results and sensitivity studies, and final discussion and error analysis are provided in Sect. 5.

2 Data and models

2.1 Satellite observations

MODerate resolution Spectroradiometer (MODIS) land surface skin temperature products together with corresponding surface albedo, emissivity, land cover, vegetation properties (leaf area index (LAI)), clouds, and aerosol optical depths are examined over global urban areas to quantify the impact of human-induced disturbances on the climate system (Jin et al. 2005a, b). This paper describes how to simulate the urban temperature effect and associated hazards.

MODIS is an advanced instrument launched in May 2000 via the US National Aeronautics and Space Administration (NASA) Earth Observing System (EOS) Terra platform. This instrument simultaneously measures atmosphere, ocean, and land surface through 36

spectral bands at 1030 LT (Terra) and 2230 LT for a given pixel. The observations used in this study (albedo, LAI, emissivity) are 1 km resolution at nadir and are scaled up to 5 km by MODIS teams, which is the best available observation. Derived from surface emission, skin temperature¹ indicates surface radiative properties and is an integrated variable related to the surface energy and water budget (Wan and Doizer 1996; Jin et al. 1997; Jin and Dickinson 1999; 2000, Jin 2004). In this work, only clear-day skin temperatures are sampled for analysis. In addition, surface emissivity is converted from MODIS spectral emissivity measurements using the MODTRAN-based spectral-to-broadband equation (Jin and Liang 2006).

The MODIS land cover product, with a 5-km resolution, is used to divide the land surface according to the International Geosphere-Biosphere Project (IGBP) 17-class land cover types (Friedl et al. 2002). The representation of urban landscapes is improved significantly with MODIS observations (Schneider et al. 2002). The MODIS BRDF/Albedo algorithm uses a three-parameter semi-empirical RossThickLiSparse-Reciprocal BRDF model to characterize the anisotropic property of land surface reflectance (Schaaf et al. 2002).

2.2 NCAR CAM2/CLM2

The urban scheme developed in this work was coupled into the existing NCAR Community Land Model Version 2 (CLM2, Dai et al. 2003; Oleson et al. 2004) and the Community Atmosphere Model Version 2 (CAM2). CLM2 is a community-developed land surface model. The detailed physical parameterization and numerical implementation is given in Oleson et al. (2004). CLM2 is designed to couple with the CAM2 atmospheric numerical model. It simulates surface albedo (direct and diffusive for visible and near-infrared spectrum), upward longwave radiation, sensible heat flux, latent heat flux, ground heat flux, water vapor flux, zonal and longitudinal stress in order to provide interactive flux boundary conditions for the overlying atmosphere model. “The model accounts for ecological differences among vegetation types, hydrological and thermal differences among soil types, and allows for multiple land cover types within one grid cell ...” (Oleson et al. 2004).

It is a well accepted approach in land surface modeling development that first examining and validating one set of parameterization in the off-line model, and then testing the parameterization in atmosphere-land surface coupled model. In this paper, first we run off-line CAM2 to examine the urban parameterization.

We then run single column model of CAM2/CLM2 (SCAM2/CLM2), partly because that single column model is computational economic than the full 3-D model; and partly because that it is relatively easier to interpret the changes in terms of parameterization processes in single column model than in a full model. The initial conditions and boundary conditions used to run SCAM2/CLM2 were derived from NCEP reanalysis, and were provided by NCAR developer in the SCAM2/CLM2 package.

¹ Previously, urban effects have been primarily indicated by urban-to-rural surface air temperature differences, namely the Urban Heat Island (UHI) effect (Oke 1976; Landsberg 1975). In this paper, satellite land surface skin temperature is examined. Skin temperature, retrieved from upward longwave radiation, is closely related to the surface radiative properties and is more suitable than the conventional surface air temperature in studies of climate change (Jin et al. 1997; Jin and Dickinson 1999, 2000, 2002), since the latter has shortcomings such as irregular spatial coverage, site changes, and coarse resolutions (Karl et al. 1988).

3 Urban scheme

3.1 Physical parameter modifications

The first step in our development of the urban scheme is to use satellite or in situ observations to identify the surface physical parameters which have been modified by urbanization. In particular, these parameters include: surface albedo, surface emissivity, leaf area index, heat capacity, thermal conductivity, and hydraulic conductivity. For example, globally averaged MODIS-measured broadband albedo product show that urban albedo differs from other surfaces, with a peak value of 0.30 over 0.9–0.12 μm , while albedos for evergreen broadleaf forests and cropland are higher and needleleaf forest albedos are lower. Earlier study suggests that realistic albedo data is needed to properly represent the surface energy budgets when the land surface is urban because urban albedo is changed by 4–10% due to the change of surface vegetation cover, paved road, and cavity effect induced by dense building regions (Jin et al. 2005a). The most unique fact in cities is that in some well-watered sub-urban regions the surface albedo may decrease while in other sub-regions like high way, the surface albedo may increase. Similarly, emissivity in general decreases from that of cropland by 2–5% (not shown, see Jin et. al. 2005a; Jin and Liang 2006).

As an example of MODIS-derived land cover properties and their ability to represent urban areas, Fig. 1 illustrates the MODIS-derived land cover for East Asia, including the large urban area surrounding Beijing, China. In order to better identify regions with significant UHI effects, daytime and nighttime surface skin temperature for Beijing and the surrounding non-urban regions are shown in Fig. 2. Evidently, UHI is observed for both July and January at daytime and at night, with a higher magnitude up-to 12°C in July daytime and 1–2°C in January night.

3.2 Urban physical process representation

Two key processes that result in strong additional terms in the energy budget Eq. 1 must be represented in an urban scheme. These are the anthropogenic heat flux and the storage heat flux.

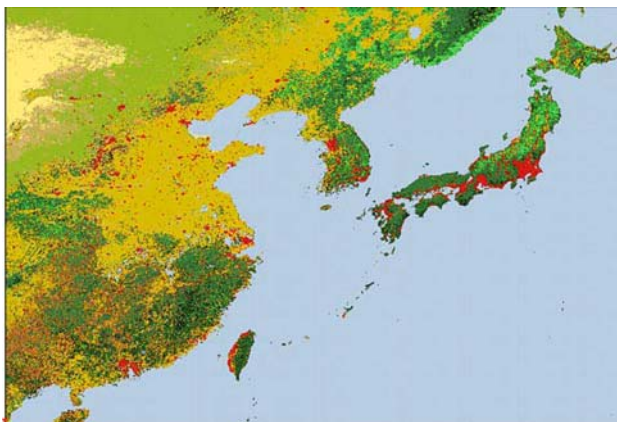


Fig. 1 Land cover observed from MODIS for East Asia. The red color represent urban. (This figure is provided by Michael D. King of NASA)

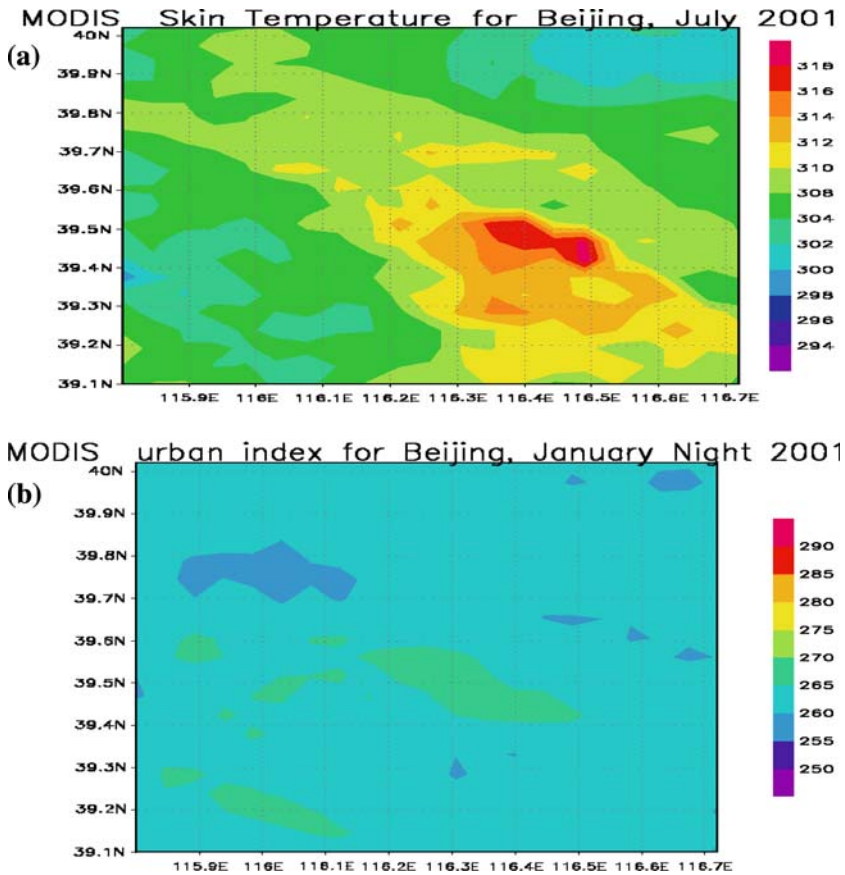


Fig. 2 (a) Urban skin temperature for Beijing region for July 2001, daytime. (b) Urban heat island effect for Beijing January 2001, nighttime. Beijing centers at (39.5N, 116E). (see Jin et al. 2005 for the definition of urban index)

3.2.1 Anthropogenic heat flux (Q_f)

As discussed by Voogt and Grimmond (2000), Q_f exhibits both seasonal and diurnal variations, and may be estimated from the following equations:

$$Q_f(\text{hour}) = Q_{f0} \{1 - 0.6 \cdot \cos(p \cdot (\text{hour} - 3)/12)\}, \tag{2}$$

where, $Q_{f0} = 62.5 \text{ W/m}^2$ in January and $Q_{f0} = 37.5 \text{ W/m}^2$ in July. ‘hour’ is the hourly time of interest. In fact, Q_{f0} is the function of human population density in the city as well as the style of human transport. Therefore, Q_{f0} varies with city, with range between 37.5 and 62.5 W/m^2 .

3.2.2 Storage heat flux (Q_s)

The storage heat flux is represented here following Arnfield (1982) and Grimmond and Oke (1999), as:

$$Q_s = S(a_i Q^* + b_i Q_s + c_i) A_i, \tag{3}$$

where a_i , b_i , and c_i are empirical coefficients corresponding to surface type. A_i is the surface area for each urban land surface type, which can be obtained from MODIS land cover data (Schneider et al. 2002); Q^* is the net radiation; and Q_s is the absorbed surface solar radiation. Details of selection a_i , b_i , c_i can be found in Grimmond and Oke (1999).

3.3 Urban roughness length parameterization

Rough urban surfaces have significant impacts on the scale and intensity of turbulence, and the closely related aerodynamic conductance for momentum. A parameterization that uses height and areal fraction (f) to calculate roughness length has been adopted from Raupach (1992). The frontal index is defined by mean height Z_h (Raupach 1992):

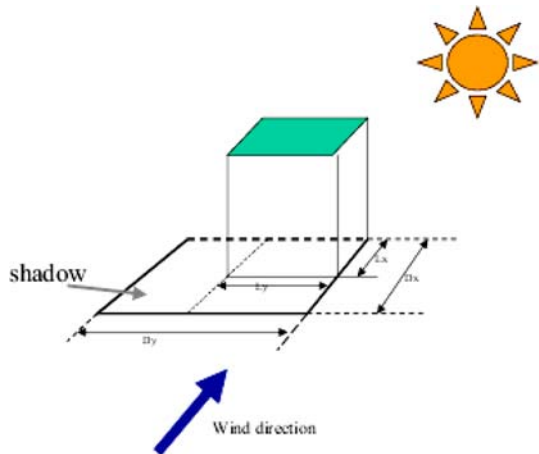
$$f = L_y Z_h (D_x D_y) \tag{4}$$

where D_x , D_y , are the characteristic length scales of buildings as shown in Fig. 3. Following the approach provided by Macdonald et al. (1998), and Eq. 4 above, we may estimate the ratio of the roughness length Z_o to the average building height Z_h as:

$$Z_o/Z_h = \left\{ (1 - Z_d/Z_h) \exp \left[- \left\{ 0.5 C_d / k^2 * (1 - Z_d/Z_h) \beta \right\} * f \right] \right\}^{-0.5}, \tag{5}$$

where Z_d is the zero-plane displacement height, C_d is a drag coefficient, k is the von Karman's constant, and β is a correction factor for the drag coefficient. Macdonald et al. (1998) showed that for staggered arrays of cubes a, β can be estimated as $\beta = 4.43$ and $\beta = 1.0$.

Fig. 3 Definitions of building length used in Eq. 4



4 Results

Figure 4 shows the concept of coupling the urban scheme in a GCM. The urban scheme is relatively independent and therefore can be easily coupled in any existing land surface model. In a GCM/Land surface model framework, the atmosphere model (in our case, CAM2) calculates atmosphere forcing that are needed by a land surface model (e.g., CLM2): surface air temperature, solar radiation, downward longwave radiation, wind, relative humidity, and precipitation. Once the land surface is called for specific gridpoint, the model needs to examine whether this gridpoint is urban or includes a fraction of urban land. If so, the newly-developed urban scheme will be called to calculate the urban surface; if not, the regular land surface model will be called. The land surface model/urban scheme then calculates sensible heat flux, latent heat flux, upward long wave radiation, and reflected solar radiation and sends the information back to the atmosphere model.

4.1 Offline CLM-urban scheme results

Our urban scheme is first incorporated in the offline CLM2. In this case, the atmosphere forcing is from NCAR/NCEP reanalysis provided by the standard NCAR CLM2 offline package. To avoid spin-up issues, we chose the NCAR recommended restart file for initial and boundary conditions. MODIS monthly mean albedo, emissivity, and LAI data are used in the model.

The urban scheme described above was implemented first offline with CLM2 for Houston, TX, and here we present the results for a “typical” day in September 2001. Figure 5 shows that the diurnal variation of ground temperature (T_G) differs in the control run (without urban scheme) and in the urban run, with the maximum around 3°C in 15:00 LT, and the minimum around 1°C in middle morning (10:00 LT) and early night (20:00 LT). The urban scheme-simulated T_G is always larger than the control case, proving that urban physical processes result in a net effect of improving surface ground temperature, namely the so-called UHI. In addition, both runs give reasonable diurnal cycles of T_G , suggesting the reliability of CLM2 and CLM2-urban model. Note the original diurnal

Fig. 4 The data flow of urban scheme coupled with CAM2/CLM2. See text for details

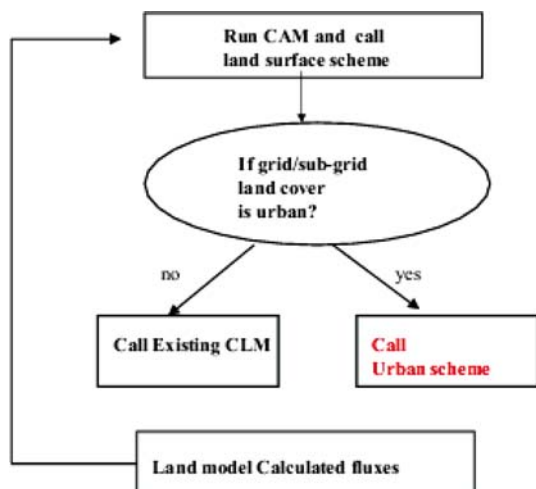
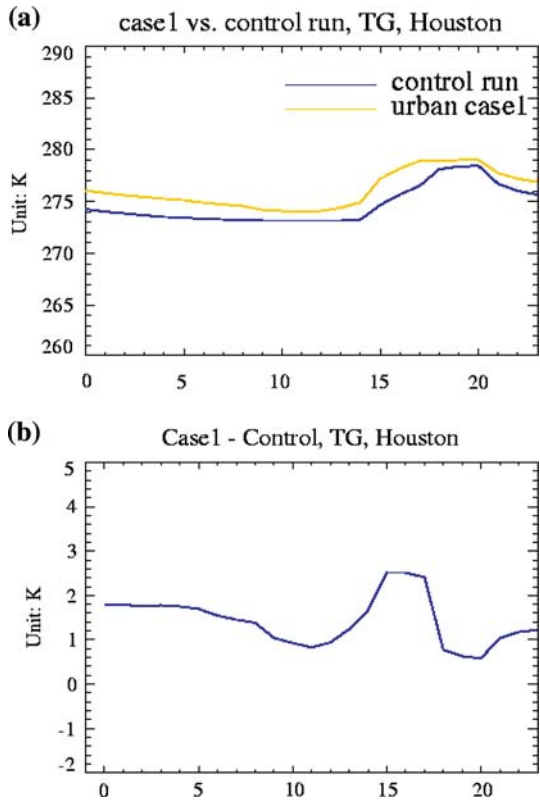


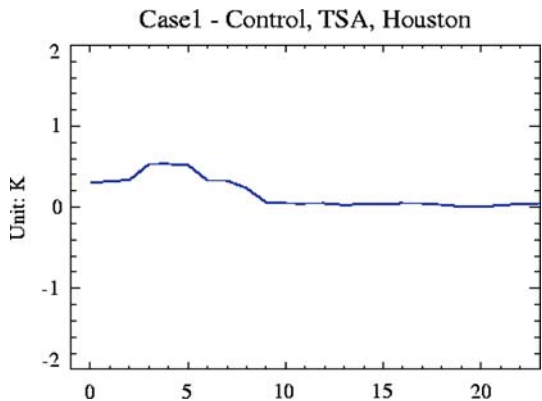
Fig. 5 (a) Diurnal cycle of surface air temperature simulations from offline CLM2-urban model. ‘‘Case 1’’ is the run with urban scheme, and ‘‘control run’’ is the CLM2 without urban scheme. (b) is the differences between case 1 and control runs. The day is one random day in September



range for T_G of Houston in September is about 5°C (Fig. 5a), and thus an increase of 3°C due to UHI is a strong change.

Figure 6 shows the differences between the control run and urban-case run for 2-m surface air temperature (T_{air}). The urban-induced change occurs at night, about 0.6°C at most. This may suggest one important feature of the UHI, namely, that the urban effect on ground temperature (T_G , Fig. 5) is different from the effect on T_{air} . For T_{air} , the urban

Fig. 6 The differences of surface air temperature simulations from offlineCLM2-urban model. ‘‘Case 1’’ is the run with urban scheme, and ‘‘control run’’ is the CLM2 without urban scheme



effect is larger during nighttime than at daytime, while T_G is changed by urbanization mostly at daytime. This is consistent with previously well-known UHI results: Previously, based on the WMO observed T_{air} data, the UHI was found most pronounced at night, and thus UHI was considered a “nocturnal phenomena” (Oke 1982). The difference between T_G and T_{air} may be caused by the physical and geometric differences of ground and 2-m air layer: During the daytime of September, the ground is heated by absorbing surface insolation. The warmed surface then transports energy in sensible heat and radiative heat back to overlying air and thus heats the air there. At night, however, the stable boundary layer maintains a warmed air layer and thus the UHI effect is evident.

Figure 7 shows the corresponding sensible heat flux (SH). Urban effect on SH is higher during the day than that during the night, peaking around 15:00 LT and minimizing at late night or early morning (5:00 LT). Urbanization always increases SH because the urban human-induced surfaces (building walls, paved roads, roofs) are water-permeable, therefore less moisture available from surface. Consequently, more partitioning of absorbed solar radiation goes to SH instead of latent heat flux (LH). During a normal day of September, the highest SH is 60 Wm^{-2} —which is about a 25% increase due to urbanization. Similarly, urbanization effects on absorbed surface solar radiation are about 8 Wm^{-2} around 15:00 LT (not shown). During this day of September, the absorbed solar radiation is from up to 250 Wm^{-2} .

The upward longwave radiation (FIRA) increases due to the urbanization-induced surface temperature increase, from $0\text{--}5 \text{ Wm}^{-2}$ (Fig. 8), with the maximum occurring at

Fig. 7 Same as Fig. 5, except for sensible heat flux

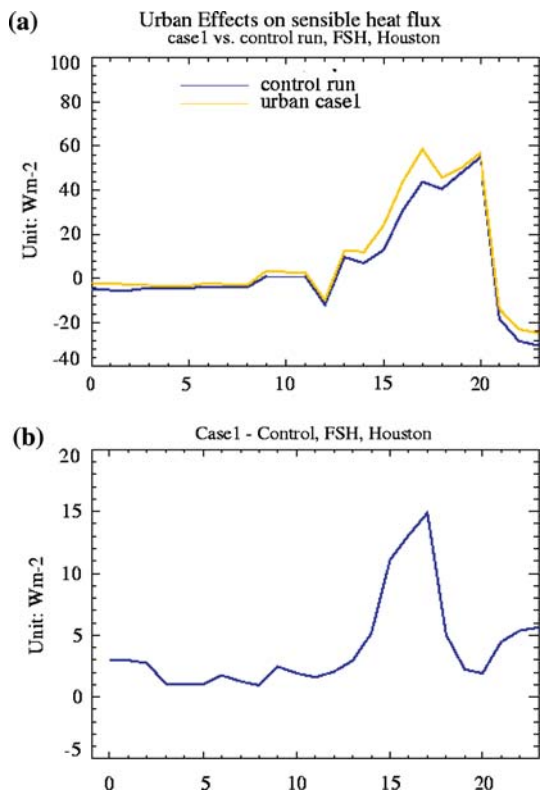
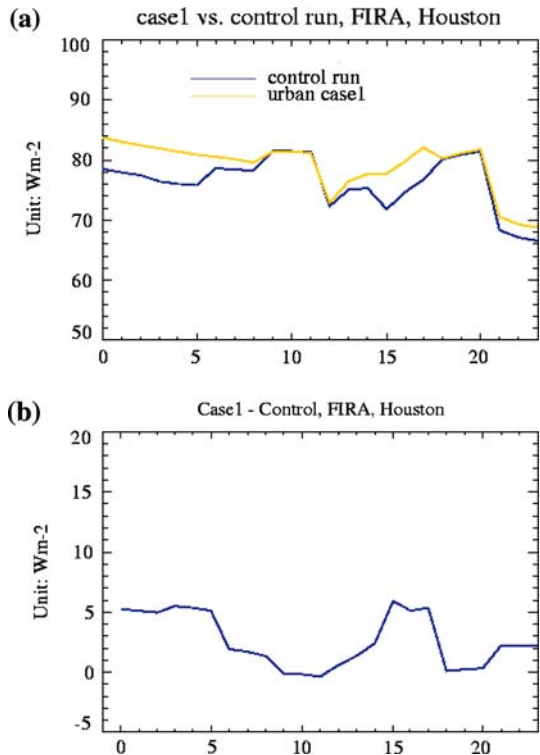


Fig. 8 Same as Fig. 7, except for upward longwave radiation, FIRA



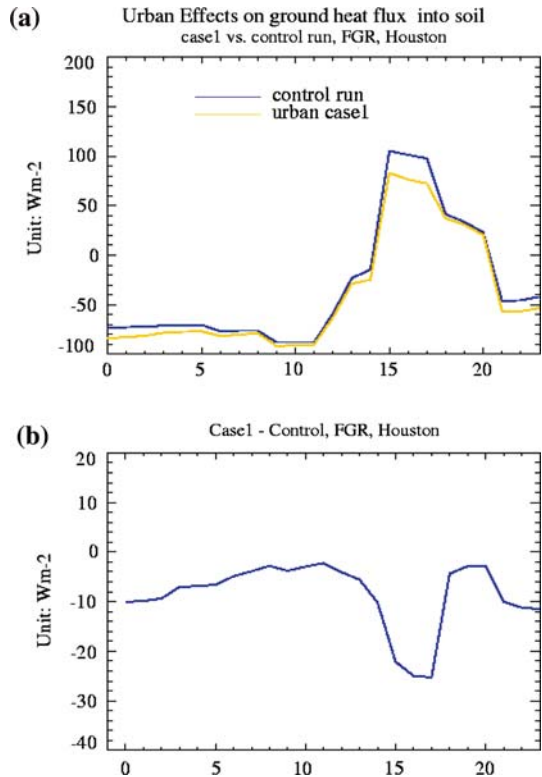
15:00 LT and late to early morning. By contrast, the ground heat flux has two low values (Fig. 9): One is during the daytime afternoon, where SH is very important. The urbanization decreases ground heat flux. Another minimum time is at the late evening (24:00 LT), about $10 Wm^{-2}$.

Anthropogenic heat flux (Q_f in Eq. 2) is $42 Wm^{-2}$ on daily average with peak up to $46 Wm^{-2}$. By comparison, the daily heat storage flux (Q_s in Eq. 3) is about $20 Wm^{-2}$, with much clearer diurnal cycle corresponding to solar radiation. The details of the coefficients in Eq. 3 need to be further examined using field experiments.

4.2 Single-column CAM2/CLM2-urban scheme results

The UHI is a combined effect of land surface and atmosphere interaction. For the second part of our study, we execute the coupled CLM2-urban model with the CAM2 single column model, to simulate the clouds, precipitation, and surface heat fluxes over Houston for January for further examination of how urban surfaces and the atmosphere interact. Figure 10 shows one day when convective clouds and convective rainfall are present. Figure 10a shows that during this cloudy day, urban effects on T_{skin} are not as significant as clear days: only at night before the rainfall occurs, T_{skin} is slightly higher than that of non-urban case (i.e., control case). Figure 10b shows the diurnal variation of convective clouds. Urban surface increases convective clouds and shifts the peak time to a latter time of the afternoon, from 64% at 10:00 LT (the 30 time steps) to 80% at 12:00–13:30 LT (40–50 time steps), although at the 14:00 LT the non-urban case had an abrupt increase in

Fig. 9 Same as Fig. 8, except for ground heat flux



clouds amount to 100%, but only lasts for a short period of time. Correspondingly, the convective rainfall amount increased and the peak time of the rainfall also delayed to a later time of the afternoon (Fig. 10c). The height of the planetary boundary layer (PBL, Fig. 10d) is increased about 100 m at night, but is the same during the day partly because both cases are cloudy and thus the heat island effect is not clear during the daytime. Sensible heat flux (Fig. 10e) is the same for the two cases because the T_{skin} change is negligible and under a cloudy day, 2-m surface air temperature is close to surface T_{skin} , which is consistent with previous understanding (Jin et. al. 1997, Jin and Dickinson 2000). By contrast, the latent heat flux (LE, Fig. 10f) shows large differences between the urban and non-urban cases, which is related to the large differences in convective rainfall. When more rainfall occurs, the land surface soil moisture or intercepted surface waters are adequate, and thus a larger part of the absorbed solar radiation is used to evaporate water than over dry surfaces.

5 Validation

Measuring urban surface heat fluxes is extremely difficult because of the highly heterogeneous urban surface. It is still an unsolved scientific question as to what is the best way to measure urban surface fluxes which can represent the integrated urban surface. Consequently, no reliable flux measurements are available to be compared with the urban scheme, which is designed to represent the integrated urban climatology instead of smaller

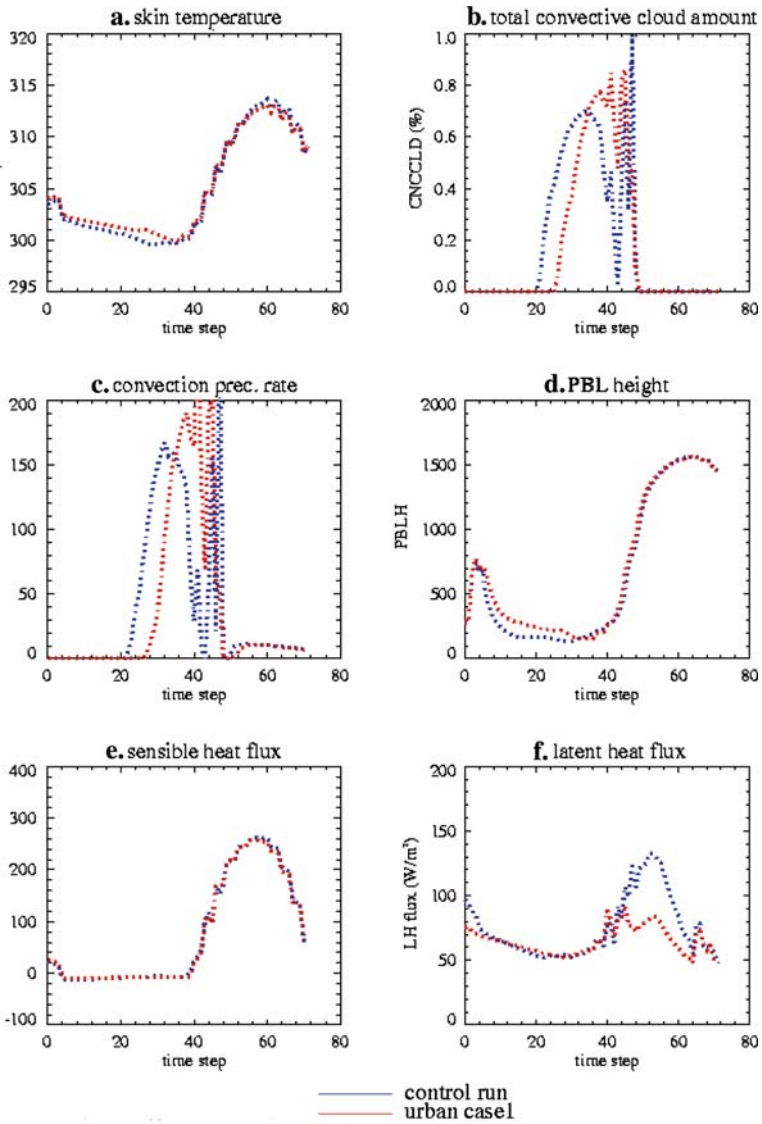


Fig. 10 Urban effects simulated from single column model of NCAR CAM2/CLM2 coupled with urban scheme: (a) Land surface skin temperature, (b) total convective cloud amount; (c) convection precipitation rate; (d) PBL height; (e) sensible heat flux; (f) latent heat flux

urban sub-types (like roofs, or parking lots). Nevertheless, quantitatively we still can evaluate the model using satellite-observed skin temperature for UHI. For example, for the clear day, UHI can be 1°C during the January night and 12°C during the July daytime (Fig. 1) (Jin et al. 2005a), the modeled UHI is within this magnitude. In addition, satellite observations disclose the shift on urban rainfall peaking time (Burian and Shepherd 2005), which is also captured in the urban scheme (Fig. 10c). Such encouraging agreement suggests that, for the first order approximation, the urban scheme may adequately represent the heat and water processes in the urban climate system.

6 Discussion

The urban temperature hazard is simulated using an offline model with the NCAR CLM2 and coupled with the single column NCAR CAM2/CLM2, respectively, to assess the mechanisms and effects of the UHI. There are two-steps in our model development. First, satellite observations of albedo, emissivity, LAI, and in situ observed thermal properties are incorporated into the current CLM2 to represent the first-order urban effects. Modified special formulations for anthropogenic heat flux, storage heat flux, and roughness length for urban areas are included in the model. Our work suggests that human activities decrease urban surface albedo and emissivity, enhance overlying atmospheric instability and convective rainfall, and eventually result in urban heat island effect. Among others, albedo seems to be the most significant factor for UHI.

It has been argued that including urban areas in GCMs is not necessary because city size by itself is too small for a GCM grid cell. However, our studies (Jin et al. 2005a) show that over large, dense urbanization regions, the size of urban regions increases dramatically to be comparable with global model grid cells. In addition, land surface models are now being coupled with GCMs as well as regional climate and weather models. For example, CLM2 is coupled to CAM as well as to regional models such as MM5 and WRF (F. Chen, personal communication 2004). Therefore the next generation of land models needs to include urban landscapes. More importantly, although a single urban region may not result in a large impact on global climate, the collective impact of all urban regions on the global climate system is as yet unknown and unstudied. Jin et al. (2005a) show that zonal mean UHI has 1–3 degree warming over the Northern Hemisphere latitudes, implying that the collective UHI may be a significant contributing factor in the overall global warming signal.

The current urban scheme does not include potentially important urban land-atmosphere feedbacks, in particular, urban aerosols' impacts on surface insolation and aerosol-cloud-rainfall interactions over urban regions. Therefore, the presented urban impacts are limited to those resulting from changes in the urban surface only. Future model development on coupled urban land-atmosphere interactions is essential for fully understanding the extent of urban impacts.

Acknowledgments We thank the Year 2003 NASA GSFC DDF, EOSIDS, and the TRMM program for supporting the initial study of this work. We also thank Robert E. Dickinson for extremely useful discussion on urban roughness length. Thanks go to our NASA Academy summer student, Mr. Miguel Roman-Colon, who helped assess early versions of the MODIS products.

References

- Arnfield AJ (1982) An approach to the estimation of the surface radiative properties and radiation budgets of cities. *Phys Geogr* 3:97–122
- Bornstein R, Lin Q (2000) Urban heat islands and summertime convective thunderstorms in Atlanta: Three case studied. *Atmos Env* 34:507–516
- Burian SJ, Shepherd JM (2005) Effects of urbanization on the diurnal rainfall pattern in Houston: Hydrological Processes: special issue on rainfall and hydrological processes 19:1089–1103
- Burian SJ, Shepherd JM, Hooshalsadat P (2004) Urbanization impacts on Houston rainstorms. In: James W (ed) *Innovative Modeling of Urban Water Systems*. BPR, 1–22
- Dai Y, Zeng X, Dickinson RE, Baker I, Bonan G, Bosilvich M, Denning S, Dirmeyer P, Houser P, Niu G, Oleson K, Schlosser A, Yang Z (2003) The Common Land Model (CLM). *Bull Am Meteorol Soc* 84:1013–1023
- Friedl MA, McIver DK, Hodges JC, Zhang Y, Muchoney D, Strahler AH, Woodcock CE, Gopal S, Schneider A, Cooper A, Baccini A, Gao F, Schaaf CB (2002) Global land cover mapping from MODIS: Algorithms and early results. *Remote Sensing Environ* 83:287–302

- Grimmond CSB, Oke TR (1999) Heat storage in urban areas: Local-scale observations and evaluation of a simple model. *J Appl Meteorol* 38:922–940
- Hansen J, Ruedy R, Sato M, Imhoff M, Lawrence W, Easterling D, Peterson T, Karl T (2001) A closer look at United States and global surface temperature change. *J Geophys Res* 106(D20):23, 947–23, 963
- IPCC, Intergovernmental Panel on Climate Change, Climate Change (2001) *The Scientific Basis. Contribution of working group I to the Third Assessment Report of the Intergovernmental Panel on Climate Change*, edited by Houghton JT et al., 881 pp, Cambridge Univ. Press, New York
- Jauregui E (1997) Aspects of urban human biometeorology, *Int J Biometeorol* 40:58–61
- Jin M (2004) Analyzing skin temperature variations from long-term AVHRR. *Bull Am Meteor Soc* 587–600
- Jin M, Dickinson RE, Vogelmann AM (1997) A comparison of CCM2/BATS skin temperature and surface air-temperature with satellite and surface observations. *J Climate* 10:1505–1524
- Jin M, Dickinson RE (1999) Interpolation of surface radiation temperature measured from polar orbiting satellites to a diurnal cycle. Part I: without clouds. *J Geophys Res* 104: 2105–2116
- Jin M, Dickinson RE (2000) A generalized algorithm for retrieving cloudy-sky skin temperature from satellite thermal infrared radiances. *J Geophys Res* D22:27037–27047
- Jin M, Dickinson RE (2002) New observational evidence for global warming from satellite. *Geophys Res Lett* 29(10), <http://dx.doi.org/10.1029/2001GL013833>
- Jin M, Shepherd JM (2005) On including urban landscape in land surface mode—How can satellite data help? *Bull Am Meteor Soc* 86(5):681–689
- Jin M, Liang S (2006) Improving land surface emissivity parameter of land surface model in GCM. *J Climate* 19:2867–2881
- Jin M, Dickinson RE, Zhang D (2005a) The footprint of urban climate change through MODIS. *J Climate* 18(10):1551–1565
- Jin M, Shepherd JM, King MD (2005b) Urban aerosols and their interaction with clouds and rainfall: A case study for New York and Houston. *J Geophys Res* 110: D10–S20, doi:10.1029/2004JD005081
- Karl TR, Diaz HF, Kukla G (1988) Urbanization: Its detection and effect in the United States Climate Record. *J Climate* 1:1099–1123
- King MD, Menzel WP, Kaufman YJ, Tanré D, Gao BC, Platnick S, Ackerman SA, Remer LA, Pincus R, Hubanks PA (2003) Cloud and aerosol properties, precipitable water, and profiles of temperature and humidity from MODIS, *IEEE Trans. Geosci Remote Sens* 41:442–458
- Kunkel KE, Changnon SA, Reinke BC, Arritt RW (1996) The July 1995 Heat Wave in the Midwest: A Climatic Perspective and Critical Weather Factors. *Bull Am Meteorol Soc* 77(7):1507–1518
- Macdonald RW, Griffiths RF, Hall DJ (1998) An improved method for estimation of surface roughness of obstacle arrays. *Atmos Environ* 32:1857–1864
- Mölders N, Olson MA (2004) Impact of urban effects on precipitation in high latitudes. *J Hydrometeorol* 5:409–429
- Olson KW et al (2004) Technical Description of the Community Land Model (CLM), NCAR Technical Note NCAR/TN-461+STR, National Center for Atmospheric Research, Boulder, Colorado 80307–3000, 173 pp
- Oke TR (1976) City size and the urban heat island. *Atmos Environ* 7:769–779
- Oke TR (1982) The energetic basis of the urban heat island, *Quart J Roy Meteor Soc* 108:1–24
- Otte TL, Lacser A, Dupont S, Ching JK-S (2004) Implementation of an urban canopy parameterization in a mesoscale meteorological model, *J App Met* 43(11):1648–1665
- Orville RE, Huffines G, Nielsen-Gammon J, Zhang RY, Ely B, Steuger S, Phillips S, Allen S, Read W (2001) Enhancement of cloud-to-ground lightning over Houston, Texas. *Geophys Res Lett* 28(13):2597–2600
- Raupach M (1992) Drag and drag partition on rough surfaces. *Bound-Layer Meteorol* 60:375–395
- Rosenfeld D (2000) Suppression of rain and snow by urban air pollution. *Science*. 287:1793–1796
- Schaaf CB, Gao F, Strahler AH et al (2002) First Operational BRDF, Albedo and Nadir Reflectance Products from MODIS. *Remote Sens Environ* 83(1):135–148
- Shepherd JM (2005) A Review of Current Investigations of Urban-Induced Rainfall and Recommendations for the Future. *Earth Inter* 9(12):1–27
- Schneider A, Friedl MA, McIver DK, Woodcock CE (2002) Mapping urban areas by fusing multiple sources of coarse resolution remotely sensed data. *Photogramm Eng Remote Sens* 69:1377–1386
- Voogt JA, Grimmond CSB (2000) Modeling surface sensible heat flux using surface radiative temperatures in a simple urban area. *J Appl Meteorol* 39:1679–1699
- Wan Z, Dozier J (1996) A generalized split-window algorithm for retrieving land-surface temperature from space. *IEEE Trans Geo Remote Sens* 34:892–904